Available online at www.sciencedirect.com
SciVerse ScienceDirect
Ceramics International 39 (2013) 6619–6622
CERAMICS INTERNATIONAL
www.elsevier.com/locate/ceramint

Piezoelectric behavior of $(1-x)K_{0.50}Na_{0.50}NbO_3-xBa_{0.80}Ca_{0.20}ZrO_3$ lead-free ceramics

Tao Chen[a,*], Hongli Wang[b], Ting Zhang[a], Guangchang Wang[a], Jifang Zhou[a], Jianwei Zhang[a], Yuhong Liu[a]

[a]*Teaching and Research Section of Physics, Chengdu Medical College, Chengdu 610083, PR China*
[b]*Teaching and Research Section of Chemistry, Chengdu Medical College, Chengdu 610083, PR China*

Received 16 December 2012; received in revised form 11 January 2013; accepted 28 January 2013
Available online 4 February 2013

Abstract

$(1-x)K_{0.50}Na_{0.50}NbO_3$–$xBa_{0.80}Ca_{0.20}ZrO_3$ [(1−*x*)KNN–*x*BCZ] lead-free ceramics were prepared by the conventional solid-state method, and the effect of BCZ content on their phase structure and piezoelectric properties was studied. A coexistence of rhombohedral–orthorhombic phases was identified in the range $0.04<x<0.08$. With increasing the BCZ content, their grain size becomes smaller, and their Curie temperature gradually decreases. An optimum piezoelectric behavior of $d_{33}\sim197$ pC/N and $k_p\sim40.6\%$ was demonstrated in the ceramic with $x=0.06$ because of the coexistence of two phases. As a result, the introduction of BCZ could further improve piezoelectric properties of KNN ceramics.

Keywords: C. Piezoelectric properties; (K, Na)NbO_3; Lead-free ceramics

1. Introduction

Lead-based piezoelectric ceramics have been extensively applied in actuators, sensors, transducers, and surface acoustic wave devices [1,2]. However, it is an urgent task to replace lead-based materials by using lead-free ones because of the toxicity of lead oxide during the preparation process [3–19]. (K, Na)NbO_3 (KNN) materials have been recently given considerable attention because of their good piezoelectric constant (d_{33}), a high Curie temperature (T_c), and environmental friendliness [3,4,7–17], which are considered as a promising candidate in the field of lead-free piezoelectric ceramics. However, it is difficult to obtain dense KNN ceramics with a high d_{33} value by using the conventional sintering method [3,4]. Some attempts have been used to improve the density and piezoelectric properties of KNN-based ceramics, such as preparation method [7], ion substitution [8–17], and so on. Among these, it is an effective way to improve their density and electrical properties by forming the phase boundary using various ABO_3 compounds, such as KNN–$LiSbO_3$ [9], KNN–$LiNbO_3$ [10], KNN–$(Bi_{0.5}Na_{0.5})TiO_3$ [14], and KNN–$BaTiO_3$ [17].

The phase boundary in functional materials is generally associated with a narrow composition region [20]. In order to construct the phase boundary in KNN ceramics, their rhombohedral–orthorhombic transition temperature ($T_{R–O}$) could be tailored to be near room temperature by doping other compositions [21]. $BaZrO_3$ (BZ) has a paraelectric phase, which can stabilize the rhombohedral phase of KNN [21]. It has been recently reported that the $T_{R–O}$ near room temperature could be induced by introducing BZ into KNN ceramics [22]. Moreover, the addition of $CaZrO_3$ could also shift the $T_{R–O}$ to be above room temperature [23]. However, there are few reports on the effect of $BaZrO_3$ and $CaZrO_3$ on the phase structure and electrical properties of KNN ceramics.

In the present work, $(1-x)K_{0.50}Na_{0.50}NbO_3$–$xBa_{0.80}Ca_{0.20}ZrO_3$ [(1−*x*)KNN–*x*BCZ] ceramics were prepared by the conventional solid-state method, and the effect of BCZ content on their phase structure and piezoelectric

*Corresponding author.
E-mail addresses: chentaocmc@163.com, myfriendsroom@163.com (T. Chen).

0272-8842/$ - see front matter © 2013 Elsevier Ltd and Techna Group S.r.l. All rights reserved.
http://dx.doi.org/10.1016/j.ceramint.2013.01.098

properties was investigated. An enhanced piezoelectric behavior was demonstrated in such a ceramic by constructing the phase boundary, and the underlying physical mechanism was also illuminated.

2. Experimental procedure

$(1-x)$KNN–xBCZ ceramics with $x=0$, 0.02, 0.04, 0.06, 0.08, and 0.10 were prepared by a conventional ceramic fabrication technique. K_2CO_3 (99.0%), Na_2CO_3 (99.8%), Nb_2O_5 (99.5%), $BaCO_3$ (99.0%), $CaCO_3$ (99.0%), and ZrO_2 (99%) were used as raw powders, and were weighed according to their stoichiometric ratio. These weighed powders were mixed in a polyethylene jar with ZrO_2 for 24 h using alcohol as a medium, then dried, and calcined at 850 °C for 4 h. Calcined powders were re-mixed, ground with PVA solution as a binder, and pressed into pellets of 10 mm in diameter and sintered at a sintering temperature of ~1110–1170 °C for 3 h in air. Silver pastes were fired at ~650 °C for 10 min on both sides of these samples as electrodes for electrical measurements. All samples were poled at a temperature of 150 °C in a silicone oil bath under a *dc* field of ~4.0 kV/mm for 20 min.

X-ray diffraction with a CuK_a radiation (XRD; D8 Advance, BrukerInc., Karlsruhe, Germany) was used to identify their phase structure. Scanning electron microscopy (SEM) was employed to study their surface microstructure. Their dielectric behavior as a function of the measurement temperature was obtained by using an LCR meter (HP 4980, Agilent, USA), and their d_{33} was measured by using a piezo-d_{33} meter (ZJ-3A, China).

3. Results and discussion

Fig. 1(a) shows the XRD patterns of $(1-x)$KNN–xBCZ ceramics in the 2θ range of 20–60°, measured at room temperature. All the ceramics have a pure perovskite phase without any secondary phases. Fig. 1(b) shows their expanded XRD patterns in the 2θ range of 42–48°. These ceramics with $x \leq 0.04$ have an orthorhombic phase, while a rhombohedral structure is observed in these ceramics with $x \geq 0.08$. Therefore, a coexistence of rhombohedral and orthorhombic phases was identified in the compositional range of $0.04 < x < 0.08$.

To study the influence of BCZ content on the microstructure of KNN ceramics, their surface morphologies were characterized by the SEM. Fig. 2(a)–(d) shows the corresponding SEM patterns of $(1-x)$KNN–xBCZ ceramics with $x=0$, 0.04, 0.06, and 0.08. All the ceramics have a dense microstructure regardless of BCZ content. Their grain size gradually decreases with increasing the BCZ content because the introduction of BCZ prohibits the grain growth of KNN ceramics, where BCZ may partly exist near the grain boundary [23].

Subsequently, we investigated the influence of BCZ content on the Curie temperature of KNN ceramics. Fig. 3 shows the temperature dependence of the dielectric constant of (1-x)KNN–xBCZ in the temperature range of room temperature ~500 °C. As shown in Fig. 3, excessive BCZ results in a relaxor behavior of KNN ceramics [22,23]. The inset in Fig. 3 plots their T_c and $T_{o\text{–}t}$ values as a function of BCZ content. These T_c and $T_{o\text{–}t}$ values decrease with increasing the BCZ content [22,23]. Their T_c value almost linearly decreases with increasing x, while it is still above room temperature, confirming that these ceramics with $x \geq 0.08$ belong to a ferroelectric rhombohedral phase rather than a paraelectric cubic phase (Fig. 1).

Fig. 4 plots the k_p, d_{33}, and Q_m values of $(1-x)$KNN–xBCZ ceramics as a function of BCZ content. An improved piezoelectric behavior of d_{33}~197 pC/N and k_p~40.6% was observed in the ceramic with $x=0.06$, and their Q_m value

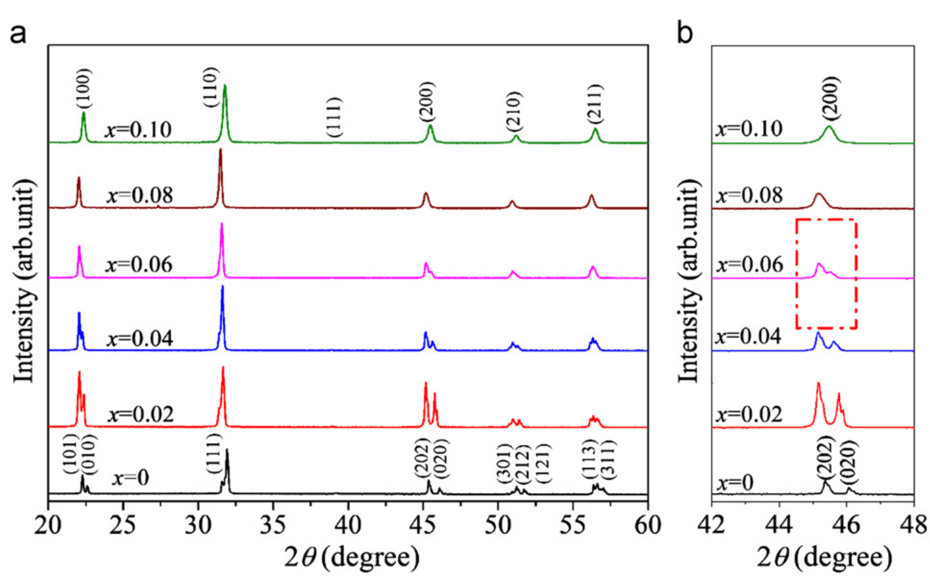

Fig. 1. (a) XRD patterns of $(1-x)$KNN–xBCZ ceramics, and (b) expanded XRD patterns of $(1-x)$KNN–xBCZ ceramics.

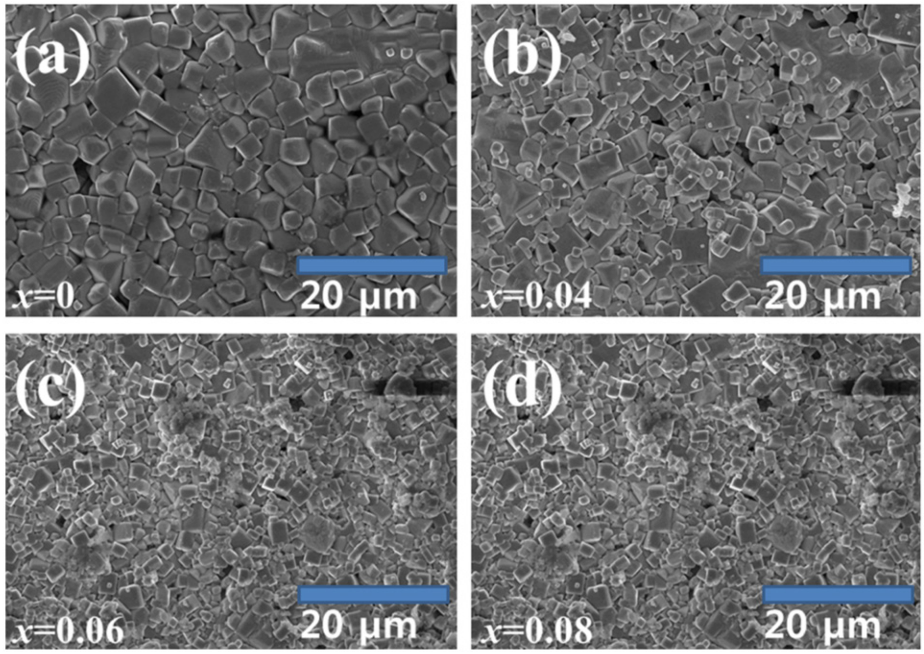

Fig. 2. SEM patterns of $(1-x)$KNN–xBCZ ceramics with (a) $x=0$, (b) $x=0.04$, (c) $x=0.06$, and (d) $x=0.08$.

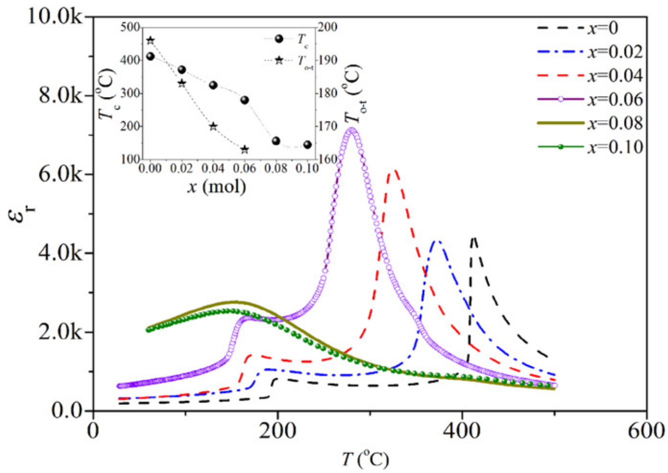

Fig. 3. Temperature dependence of the dielectric constant of $(1-x)$KNN–xBCZ ceramics, the inset is their Tc and To-t as a function of BCZ content

gradually decreases with increasing the BCZ content. In this work, the d_{33} value of ~ 197 pC/N is much higher than those of pure KNN ceramics prepared by a hot pressing or a spark plasma sintering [4,24], and is also higher than that of KNN–$CaZrO_3$–$LiNbO_3$ ceramics with $T_{R\text{–}O}$ [25], as shown in Table 1. It is well known that the phase boundary strongly affects piezoelectric properties of KNN-based ceramics [9,10,14,17,20,22,23], such as an orthorhombic–tetragonal phase transition [9,10,13], a rhombohedral–tetragonal phase transition [22,23], and a rhombohedral and orthorhombic phase transition [21,25]. In this work, a $T_{R\text{–}O}$ was involved in (1–x)KNN–xBCZ with $x=0.06$. As a result, an enhanced d_{33} value of ~ 197 pC/N could be largely due to the involvement of such a $T_{R\text{–}O}$ in the ceramic with $x=0.06$ because of the involvement of more possible polarization states.

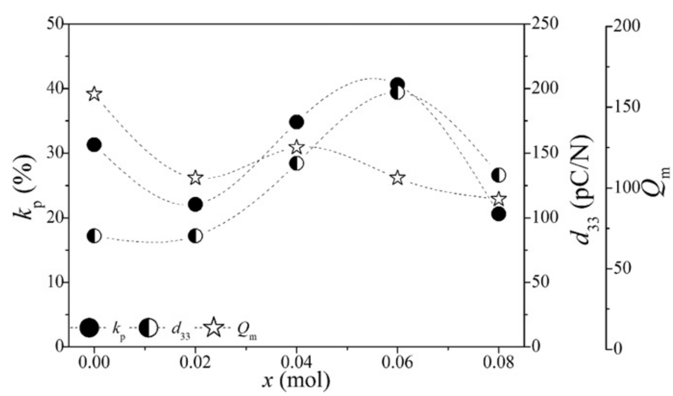

Fig. 4. Piezoelectric properties and mechanical coupling factor of $(1-x)$KNN–xBCZ ceramics as a function of BCZ content.

Moreover, a dense microstructure may partly improve its piezoelectric properties.

4. Conclusions

$(1-x)$KNN–xBCZ ceramics were prepared by the conventional solid-state method. A coexistence of rhombohedral and orthorhombic phases was detected in the range of $0.04 < x < 0.08$. The introduction of BCZ results in the decrease of the grain size and a denser microstructure. Moreover, their Curie temperature also decreases with increasing the BCZ content. The ceramic with $x=0.06$ has an enhanced piezoelectric behavior of $d_{33} \sim 197$ pC/N and $k_p \sim 40.6\%$ because of the coexistence of two phases at room temperature.

Table 1
Properties of KNN-based piezoelectric ceramics.

Material systems	d_{33} (pC/N)	k_p	T_c (°C)	Reference
KNN	80	0.360	—	[4]
KNN (SPS)	148	0.390	—	[24]
KNN–$CaZrO_3$–$LiNbO_3$	145	0.332	~320	[25]
0.94KNN–0.06BCZ	197	0.406	~281	In this work

Acknowledgments

Authors gratefully acknowledge the support of the Chengdu Medical College.

References

[1] T. Kimura, Application of texture engineering to piezoelectric ceramics—a review, Journal of the Ceramic Society of Japan 114 (2006) 15–25.
[2] C.C.M. Wu, M. Kahn, W. Moy, Piezoelectric ceramics with functional gradients: a new application in material design, Journal of the American Ceramic Society 79 (1996) 809–812.
[3] G. Shirane, R. Newnham, R. Pepinsky, Dielectric properties and phase transitions of $NaNbO_3$ and (Na, K)NbO_3, Physical Review 96 (1954) 581–588.
[4] R.E. Jaeger, L. Egerton, Hot pressing of potassium–sodium niobates, Journal of the American Ceramic Society 45 (1962) 209–213.
[5] W.F. Liu, X.B. Ren, Large piezoelectric effect in Pb-free ceramics, Physical Review Letters 103 (2009) 257602.
[6] J. Wu, D. Xiao, W. Wu, Q. Chen, J. Zhu, Z. Yang, J. Wang, Role of room-temperature phase transition in the electrical properties of (Ba, Ca)(Ti, Zr)O_3 ceramics, Scripta Materialia 65 (2011) 771–774.
[7] Y. Saito, H. Takao, T. Tani, T. Nonoyama, K. Takatori, T. Homma, T. Nagaya, M. Nakamura, Lead-free piezoceramics, Nature 432 (2004) 84–87.
[8] S.J. Zhang, R. Xia, T.R. Shrout, Modified $(K_{0.5}Na_{0.5})NbO_3$ based lead-free piezoelectrics with broad temperature usage range, Applied Physics Letters 91 (2007) 132913.
[9] J.G. Wu, Y.Y. Wang, D.Q. Xiao, J.G. Zhu, P. Yu, L. Wu, W.J. Wu, Piezoelectric properties of $LiSbO_3$–modified $(K_{0.48}Na_{0.52})NbO_3$ lead-free ceramics, Japanese Journal of Applied Physics 46 (2007) 7375–7377.
[10] Y. Guo, K. Kakimoto, H. Ohsato, Phase transitional behavior and piezoelectric properties of $(Na_{0.5}K_{0.5})NbO_3$–$LiNbO_3$ ceramics, Applied Physics Letters 85 (2004) 4121–4213.
[11] J.G. Wu, D.Q. Xiao, Y.Y. Wang, W.J. Wu, B. Zhang, J. Li, J.G. Zhu, $CaTiO_3$–modified $[(K_{0.5}Na_{0.5})_{0.94}Li_{0.06}](Nb_{0.94}Sb_{0.06})O_3$ lead-free piezoelectric ceramics with improved temperature stability, Scripta Materialia 59 (2008) 750–752.
[12] M. Matsubara, T. Yamaguchi, W. Sakamoto, K. Kikuta, T. Yogo, S. Hirano, Processing and piezoelectric properties of lead-free (K, Na)(Nb, Ta)O_3 ceramics, Journal of the American Ceramic Society 88 (2005) 1190–1196.
[13] J.G. Wu, D.Q. Xiao, Y.Y. Wang, J.G. Zhu, L. Wu, Y.H. Jiang, Effects of K/Na ratio on the phase structure and electrical properties of $(K_xNa_{0.96-x}Li_{0.04})(Nb_{0.91}Ta_{0.05}Sb_{0.04})O_3$ lead-free ceramics, Applied Physics Letters 91 (2007) 252907.
[14] R.Z. Zuo, X.S. Fang, C. Ye, Phase structures and electrical properties of new lead-free $(Na_{0.5}K_{0.5})NbO_3$–$(Bi_{0.5}Na_{0.5})TiO_3$ ceramics, Applied Physics Letters 90 (2007) 092904.
[15] H.L. Du, W.C. Zhou, F. Luo, D.M. Zhu, S.B. Qu, Z.B. Pei, Perovskite lithium and bismuth modified potassium–sodium niobium lead-free ceramics for high temperature applications, Applied Physics Letters 91 (2007) 182909.
[16] J. Rödel, W. Jo, K. Seifert, E.-M. Anton, T. Granzow, Perspective on the development of lead-free piezoceramics, Journal of the American Ceramic Society 92 (2009) 1153–1177.
[17] E.Z. Li, H. Kakemoto, S. Wada, T. Tsurumi, Enhancement of Q_m by co-doping of Li and Cu to potassium sodium niobate lead-free ceramics, IEEE Transactions on Ultrasonics, Ferroelectrics and Frequency Control 55 (2008) 980–987.
[18] Z.P. Yang, B. Liu, L.L. Wei, Y.T. Hou, Structure and electrical properties of $(1-x)Bi_{0.5}Na_{0.5}TiO_3$–$xBi_{0.5}K_{0.5}TiO_3$ ceramics near morphotropic phase boundary, Materials Research Bulletin 43 (2008) 81–89.
[19] C.R. Zhou, X.Y. Liu, Dielectric and piezoelectric properties of bismuth-containing complex perovskite solid solution of $Bi_{1/2}Na_{1/2}TiO_3-Bi(Mg_{2/3}Nb_{1/3})O_3$, Journal of Materials Science 43 (2008) 1016–1019.
[20] D.E. Cox, B. Noheda, G. Shirane, Y. Uesu, K. Fujishiro, Y. Yamada, Universal phase diagram for high-piezoelectric perovskite systems, Applied Physics Letters 79 (2001) 400–402.
[21] R.P. Wang, H. Bando, T. Katsumata, Y. Inaguma, H. Taniguchi, M. Itoh, Tuning the orthorhombic–rhombohedral phase transition temperature in sodium potassium niobate by incorporating barium zirconate, Physica Status Solidi RRL 3 (2009) 142–144.
[22] R. Zuo, J. Fu, Rhombohedral–tetragonal phase coexistence and piezoelectric properties of (Na K)(Nb Sb)O_3–$LiTaO_3$–$BaZrO_3$ lead-free ceramics, Journal of the American Ceramic Society 94 (5) (2011) 1467–1470.
[23] W. Liang, W. Wu, D. Xiao, J. Zhu, Construction of new morphotropic phase boundary in $0.94(K_{0.42-x}Na_{0.6}Ba_xNb_{1-x}Zr_x)O_3$–$0.06LiSbO_3$ lead-free piezoelectric ceramics, Journal of the American Ceramic Society 94 (12) (2011) 4317–4322.
[24] J.F. Li, K. Wang, B.P. Zhang, L.M. Zhang, Ferroelectric and piezoelectric properties of fine-grained $Na_{0.5}K_{0.5}NbO_3$ lead-free piezoelectric ceramics prepared by spark plasma sintering, Journal of the American Ceramic Society 89 (2) (2006) 706–709.
[25] W.F. Liang, W.J. Wu, D.Q. Xiao, J.G. Zhu, Effect of the addition of $CaZrO_3$ and $LiNbO_3$ on the phase transitions and piezoelectric properties of $K_{0.5}Na_{0.5}NbO_3$ lead-free ceramics, Journal of the American Ceramic Society 94 (12) (2011) 4317–4322.